

A viscoplastic model for porous single crystals containing ellipsoidal voids at finite strains

A. Mbiakop^{a,b}, K. Danas^b, A. Constantinescu^b

a. Centre de Technologies de Michelin, 63100 Ladoux, France

b. Laboratoire de Mécanique des Solides, Ecole Polytechnique de Paris, CNRS, France

Résumé :

Cette contribution présente un modèle viscoplastique grandes déformations pour des monocristaux poreux à cavités ellipsoïdales générales. Le modèle proposé est basé sur une méthode d'homogénéisation variationnelle non linéaire (MVAR) qui utilise un matériau de comparaison linéaire poreux pour estimer la réponse effective du monocristal non linéaire poreux. Spécifiquement, le modèle a étendu le nouveau modèle monocristallin poreux (Mbiakop et al. [2015b,c]) avec des relations décrivant l'évolution en grandes transformations de la microstructure (porosité, forme et orientation des pores) de monocristaux poreux aléatoires soumis à des conditions générales de chargement. Le présent modèle est ensuite utilisé pour effectuer une étude de plusieurs mécanismes microstructuraux à différents régimes de triaxialité pour plusieurs structures cristallines (BCC, HCP et FCC), différents exposants de fluage et diverses fractions volumiques initiales. En particulier le fort couplage entre l'anisotropie du cristal et l'anisotropie (morphologique) induite par la forme et l'orientation des cavités est discutée.

Abstract :

This paper presents a rate-dependent model at finite strains for porous single crystals containing general ellipsoidal voids. The proposed model is based on a nonlinear variational homogenization method (MVAR) which makes use of a linear comparison porous material to estimate the effective response of the nonlinear porous single crystal. Specifically the model extended the novel porous single crystal model (Mbiakop et al. [2015b,c]) with relations describing the evolution of microstructure (porosity, void shape and orientation) of random porous single crystals subjected to general loading conditions. The present model is then used in order to carry out an investigation of several microstructural mechanisms at different triaxiality regime for several crystal structure (BCC, HCP and FCC), different creep exponents and initial void volume fraction. In particular the strong coupling between the anisotropy of the crystal and the (morphological) anisotropy induced by the shape and orientation of the voids is discussed.

Mots clefs : Plasticité cristalline, matériaux poreux, homogénéisation, anisotropie microstructurale.

1 Introduction

Voids originating in the manufacturing process have a strong influence on the lifetime as well as deformability of materials and play a major role on the constitutive response of metallic alloys. Indeed, as recently indicated by experimental observations (Srivastava et al. [2012], Kondori and Benzerga [2014a,b]) at high enough temperatures on tensile specimens, the growth of initially present processing induced voids in a nickel based single crystal superalloy as well as in standard polycrystals played a significant role in limiting creep life. The presence of voids in metals is well known to be one of the main causes of ductile failure, as addressed in pioneering works by (Mc Clintock [1968], Rice and Tracey [1969], Gurson [1977]). The reader is referred to a recent review of Benzerga and Leblond [2010] for more completeness on the bibliography in this subject.

In the context of rate-(in)dependent anisotropic matrix systems and more specifically for phenomenological Hill-type matrix, there are fewer results in the literature (see for instance Benzerga et al. [2004], Keralavarma et al. [2011]). Porous single crystals have mainly been studied through discrete dislocations dynamics, molecular dynamics at smaller scales or using finite element simulations. These anisotropic matrix systems have known slip directions and contain generally a low volume fraction of impurities. Subjected to external loads such material systems fail or decohere leading to the creation of pores, which in turn evolve in size, shape and orientation (Srivastava and Needleman [2012]).

However, there have been only a handful of models for porous single crystals which deal with special void geometries, loading conditions and slip system orientations. Such studies involve the study of cylindrical voids with circular cross-section in a rigid-ideally plastic face-centered cubic (FCC) single crystals using slip line theory [Gan and Kysar, 2007], the study of two-dimensional “out of plane” cylindrical voids with circular cross-section subjected to anti-plane loadings [Idiart and Ponte Castañeda, 2007], that of spherical voids and general loading conditions with/without microstructure evolution [Han et al., 2013, Paux et al., 2015, Chao et al., 2016] and that of ellipsoidal voids and general loading conditions [Mbiakop et al., 2015c]. While each one of these studies has its own significant contribution to the understanding of the effective response of porous single crystals none of them is general enough in the sense of arbitrary void shapes and orientations, general loading conditions and microstructure evolution.

In this regard, the aim of the present study is to propose a finite deformation viscoplastic constitutive model for porous single crystals that is able to deal with arbitrary crystal anisotropy, arbitrary ellipsoidal void shapes at any given orientation, general loading conditions and microstructure evolution. The developed model used an appropriate extension of a former work of the authors [Mbiakop et al., 2015c] combined with relations describing the evolution of microstructure (porosity, void shape and orientation).

2 A MVAR porous single crystal model

A formulation at finite strains is proposed for porous single crystals containing ellipsoidal voids in this section. In order to achieve this goal we will first recall the instantaneous effective behavior (Mbiakop et al. [2015b,c]). Then based on the work of (Ponte Castañeda and Zaidman [1994], Danas and Aravas [2012]), we will present the relevant evolution laws for the internal microstructural variables used to describe the volume fraction, shape and orientation of the voids. In such framework, the microstructure evolves on average to ellipsoidal voids in time with different shape and orientation. At this stage, for simplicity in the homogenization procedure elasticity effects are neglected.

2.1 Microstructure

Let us consider a representative volume element (RVE) of a porous single crystals occupying a domain Ω . The material is analyzed as a two-phase composite comprising the single crystal matrix (subdomain $\Omega^{(1)}$) and the vacuous phase (subdomain $\Omega^{(2)}$). The hypothesis of separation of length scales is made and it implies that the size of the voids (microstructure) is much smaller than the size of the matrix and the variation of the loading conditions at the level of the matrix, thus allowing for the homogenization of such a material system.

In the present study, following previous work of Willis [1977], we consider a “particulate” microstructure which is a generalization of the Eshelby [1957] dilute microstructure in the non-dilute regime. More specifically, we consider a “particulate” porous material (see Fig. 1) consisting of ellipsoidal voids aligned at a certain direction, whereas the distribution function, which is also taken to be ellipsoidal in shape, provides information about the distribution of the centers of the pores. For simplicity, one will also consider that the shape and orientation of the distribution function is identical to the shape and orientation of the voids themselves (see Danas and Ponte Castañeda [2009]). Thus, as shown in Fig. 1, the internal variables characterizing the state of the microstructure are:

- The *porosity* or *volume fraction* of the voids $f = V_2/V$, where $V = V_1 + V_2$ is the total volume, with V_1 and V_2 being the volume occupied by the matrix and the vacuous phase, respectively.
- The *two aspect ratios* of the lengths of the principal axes of the representative ellipsoidal void $2a_i$ ($i = 1, 2, 3$), expressed as $w_1 = a_3/a_1$, $w_2 = a_3/a_2$ ($w_3 = 1$).
- The *orientation unit vectors* of the representative ellipsoidal void $\mathbf{n}^{(i)}$, ($i = 1, 2, 3$), defining an orthonormal basis set.

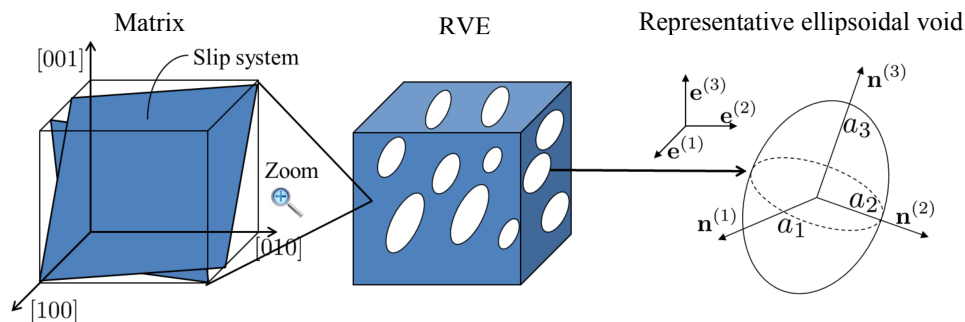


Figure 1: Representative ellipsoidal voids embedded in a crystal matrix.

The above set of the microstructural variables can then be denoted by the set

$$s_\alpha = \left\{ f, w_1, w_2, \mathbf{n}^{(1)}, \mathbf{n}^{(2)}, \mathbf{n}^{(3)} \right\} \quad (1)$$

To conclude, in the general case, where the aspect ratios and the orientation of the ellipsoidal voids are such that $w_1 \neq w_2 \neq 1$ and $\mathbf{n}^{(i)} \neq \mathbf{e}^{(i)}$, the overall porous material behavior becomes highly anisotropic. Therefore estimating its overall response is a difficult challenge.

2.2 MVAR effective estimate

In the present work, we will make use of the general, nonlinear homogenization methods developed by Ponte Castañeda [1991, 2002], which are based on the construction of a linear comparison composite

(LCC) with the same microstructure as the nonlinear composite. Using this suitably designed variational principle, it is shown in (Mbiakop et al. [2015c]) that a modified variational estimate of the effective viscoplastic stress potential of a general crystalline porous material can be defined such that

$$\tilde{U}_{mvar}(\bar{\boldsymbol{\sigma}}) = (1-f) \sum_{s=1}^K \frac{\dot{\gamma}_0^{(s)} \tau_0^{(s)}}{n+1} \left(\frac{\sqrt{\bar{\boldsymbol{\sigma}} \cdot \hat{\mathbf{S}}^{mvar,(s)} \cdot \bar{\boldsymbol{\sigma}}}}{\tau_0^{(s)} (1-f)} \right)^{n+1}, \quad (2)$$

where

$$\hat{\mathbf{S}}^{mvar,(s)} = \hat{\mathbf{S}}^{var,(s)} + (q_J^2 - 1) \mathbf{J} \cdot \hat{\mathbf{S}}^{var,(s)} \cdot \mathbf{J}, \quad q_J = \sqrt{\frac{15}{f}} \left\{ \frac{(1-f)(\beta_n)^{\frac{1}{n}}}{n(f^{-1/n} - 1)} \right\}^{\frac{n}{n+1}}, \quad \beta_n = \frac{4}{25} 6^{-\frac{n}{2}} \quad (3)$$

Here,

$$\hat{\mathbf{S}}^{var,(s)} = \frac{1}{2} \mathbf{E}^{(s)} + \frac{f}{K} \hat{\mathbf{S}}^*, \quad \mathbf{E}^{(s)} = 2\boldsymbol{\mu}^{(s)} \otimes \boldsymbol{\mu}^{(s)}, \quad \forall s = 1, K, \quad J_{ijkl} = \frac{1}{3} \delta_{ij} \delta_{kl}. \quad (4)$$

where $\boldsymbol{\mu}^{(s)}$ ($\forall s = 1, \dots, K$) is the Schmid tensor given by

$$\boldsymbol{\mu}^{(s)} = \frac{1}{2} \left(\mathbf{m}^{(s)} \otimes \mathbf{s}^{(s)} + \mathbf{s}^{(s)} \otimes \mathbf{m}^{(s)} \right), \quad (5)$$

with $\mathbf{m}^{(s)}$ and $\mathbf{s}^{(s)}$ denoting the unit vectors normal to the slip plane and along the slip direction in the s^{th} system, respectively.

In addition, $\hat{\mathbf{S}}^*$ is a microstructural tensor related to the Eshelby tensor (Eshelby [1957]). This tensor contains information on the void shape and orientation and is detailed in Mbiakop et al. [2015c].

Furthermore, we can readily determine the corresponding macroscopic strain-rate $\bar{\mathbf{D}}$ through the relation

$$\bar{\mathbf{D}} = \frac{\partial \tilde{U}_{mvar}}{\partial \bar{\boldsymbol{\sigma}}} = \sum_{s=1}^K \dot{\gamma}_0^{(s)} \left(\frac{\sqrt{\bar{\boldsymbol{\sigma}} \cdot \hat{\mathbf{S}}^{mvar,(s)} \cdot \bar{\boldsymbol{\sigma}}}}{\tau_0^{(s)} (1-f)} \right)^n \frac{\hat{\mathbf{S}}^{mvar,(s)} \cdot \bar{\boldsymbol{\sigma}}}{\sqrt{\bar{\boldsymbol{\sigma}} \cdot \hat{\mathbf{S}}^{mvar,(s)} \cdot \bar{\boldsymbol{\sigma}}}} \quad (6)$$

2.3 Evolution of microstructure at finite strains

The determination of the instantaneous effective behavior of nonlinear porous media with particulate microstructures has been carried out through a set of internal variables denoted as $s_\alpha = \{f, w_1, w_2, \mathbf{n}^{(1)}, \mathbf{n}^{(2)}, \mathbf{n}^{(3)}\}$ (see fig. 1). For completeness, it is useful to recall here that these microstructural variables correspond to the volume fraction of the voids or porosity f , the shape of the voids denoted with the two aspect ratios w_1 and w_2 , and the orientation of the principal axes of the representative ellipsoidal void, i.e., the orientation vectors $\mathbf{n}^{(i)}$, $i = 1, 2, 3$.

At this stage of the work, we neglect elasticity. This is done for simplicity but elasticity effects could be added in future studies. This implies that $\bar{\mathbf{D}} = \bar{\mathbf{D}}^p$ since $\bar{\mathbf{D}}^e = 0$, where the superscript ‘‘p’’ and ‘‘e’’ refer to plastic and elastic parts.

2.3.1 Evolution of the porosity

Next by neglecting elastic contributions, the matrix material is plastically incompressible (crystal plasticity), and thus the evolution equation for the porosity f can be obtained from mass conservation and reads (Tvergaard and Needleman [1984])

$$\dot{f} = (1 - f)\overline{D}_{ii}, \quad i = 1, 2, 3. \quad (7)$$

Furthermore, it is important to precise that void nucleation is not considered in the above relation.

2.3.2 Evolution of the aspect ratios

The evolution law for the aspect ratios is obtained by using standard kinematics and the definition $w_i = a_3/a_i$, $i = 1, 2$, such that (Ponte Castañeda and Zaidman [1994])

$$\dot{w}_i = \alpha_w w_i \left(\mathbf{n}^{(3)} \cdot \overline{\mathbf{D}}^{(2)} \mathbf{n}^{(3)} - \mathbf{n}^{(i)} \cdot \overline{\mathbf{D}}^{(2)} \mathbf{n}^{(i)} \right) = \alpha_w w_i \left(\mathbf{n}^{(3)} \otimes \mathbf{n}^{(3)} - \mathbf{n}^{(i)} \otimes \mathbf{n}^{(i)} \right) \cdot \overline{\mathbf{D}}^{(2)}, \quad (8)$$

where there is no summation on $i = 1, 2$ and $\overline{\mathbf{D}}^{(2)}$ is the average strain-rate in the void. The scalar factor α_w has been introduced in the last expression in a heuristic manner in order to enhance the accuracy of the evolution of the aspect ratios, since Danas and Aravas [2012] have showed that the original variational method and consequently the present MVAR tend to underestimate the evolution of the void shape at low stress triaxialities. The factor α_w is in general considered as a free parameter that can be calibrated from experiments.

2.3.3 Evolution of the orientation vectors

The evolution of the orientation vectors $\mathbf{n}^{(i)}$, $i = 1, 2, 3$ is determined by the spin of the Eulerian axes of the ellipsoidal voids, or microstructural spin ω , as

$$\dot{\mathbf{n}}^{(i)} = \omega \mathbf{n}^{(i)}, \quad i = 1, 2, 3 \quad (9)$$

The microstructural spin ω is related to the average spin and the average strain-rate in the void, $\overline{\boldsymbol{\Omega}}^{(2)}$ and $\overline{\mathbf{D}}^{(2)}$, by the classical kinematic relation written in direct notation

$$\omega = \overline{\boldsymbol{\Omega}}^{(2)} + \frac{1}{2} \sum_{\substack{i,j=1 \\ i \neq j \\ w_i \neq w_j}}^3 \frac{w_i^2 + w_j^2}{w_i^2 - w_j^2} \left[\left(\mathbf{n}^{(i)} \otimes \mathbf{n}^{(j)} + \mathbf{n}^{(j)} \otimes \mathbf{n}^{(i)} \right) \cdot \overline{\mathbf{D}}^{(2)} \right] \mathbf{n}^{(i)} \otimes \mathbf{n}^{(j)}, \quad w_3 = 1. \quad (10)$$

The special case in which at least two aspect ratios are equal is discussed later in this section.

An equivalent equation to deal with both void aspect ratios and rotation has been proposed by Madou and Leblond [2013].

In addition, it is useful to discuss the evaluation of the Jaumann rate of the orientation vectors $\mathbf{n}^{(i)}$, denoted by $\overset{\nabla}{\mathbf{n}}^{(i)}$, ($i = 1, 2, 3$). The Jaumann rate is related to the standard time derivative of relation (9)

by

$$\mathbf{n}^{\nabla(i)} = \dot{\mathbf{n}}^{(i)} - \overline{\Omega} \mathbf{n}^{(i)} = (\omega - \overline{\Omega}) \mathbf{n}^{(i)}, \quad i = 1, 2, 3, \quad (11)$$

with $\overline{\Omega}$ being the macroscopic average spin applied externally in the problem. At this point, it is convenient to introduce the notion of the plastic spin (Dafalias [1985]), which is defined as the spin of the continuum relative to the microstructure, i.e.,

$$\Omega^p = \overline{\Omega} - \omega. \quad (12)$$

Consequently,

$$\mathbf{n}^{\nabla(i)} = -\Omega^p \mathbf{n}^{(i)}, \quad i = 1, 2, 3. \quad (13)$$

Furthermore, we point out that special care needs to be taken for the computation of the spin of the Eulerian axes in the case of a spherical void, i.e., when $w_1 = w_2 = w_3 = 1$, as well as for a spheroidal void, i.e., when $w_1 = w_2 \neq w_3 = 1$ or $w_1 \neq w_2 = w_3 = 1$ or $w_1 = w_3 \neq w_2 = 1$. More specifically, when two of the aspect ratios are equal, the component Ω_{12}^p becomes indeterminate. Since the spin $\overline{\Omega}_{12}^p$ is inconsequential in this case, it can be set equal to zero, which implies that $\omega_{12} = \overline{\Omega}_{12}$. This notion can be applied whenever the shape of the void is spheroidal, in any given orientation. In the same way, when the voids are spherical, $\Omega^p = 0$ and hence $\mathbf{n}^{(i)} = \overline{\Omega} \mathbf{n}^{(i)}$, $i = 1, 2, 3$.

3 Results: MVAR predictions

This section is concerned with some predictions of the effective response and evolution of microstructure of random porous single crystals subjected to general loading conditions. More precisely, the evolutions laws of the microstructural variables depicted in the previous section are applied to several crystalline structures for a range of material parameters.

The matrix phases considered (single crystals) are taken to be initially unloaded with no hardening, i.e. $\tau_0^{(s)} = \tau_0$, $\forall s = 1, K$, while the voids are initially spherical with $w_1 = w_2 = 1$. The initial porosity is taken to be $f_0 = 1\%$ and the elasticity effects are neglected. It should be noted that the macroscopic response of the porous material at large deformations is strongly affected by the hardening, the viscoplastic creep exponent, the initial porosity f_0 and the initial aspect ratios w_1 and w_2 , but we will not carry out an exhaustive parametric study with respect to those parameters here. Moreover, in the following, the microstructural variables will be plotted as functions of the equivalent strain $\bar{\varepsilon}_e$ defined as

$$\bar{\varepsilon}_e = \int_t \sqrt{\frac{2}{3} \overline{\mathbf{D}}' \cdot \overline{\mathbf{D}}'} dt, \quad (14)$$

where $\overline{\mathbf{D}}'$ refers to the deviatoric part of the average strain-rate $\overline{\mathbf{D}}$.

Fig. 2 shows MVAR plots of (a) the equivalent stress $\bar{\sigma}_e$, (b) the porosity f , and the aspect ratios (c) w_1 and (d) w_2 , as a function of the equivalent strain $\bar{\varepsilon}_e$, for a BCC single crystal, a creep exponent $n = 10$, four Lode angles $\theta = 0^\circ, 20^\circ, 30^\circ, 60^\circ$ and a low value of the stress triaxiality ($X_\Sigma = 0.1$). The main observation in Fig. 2a is that there is a slight effect of the Lode angle on the overall mechanical response of the porous single crystal.

In addition, let us analyze plots for the evolution of f , w_1 and w_2 in Fig. 2bâ-d, respectively, as a function of the equivalent strain $\bar{\varepsilon}_e$. In graph. 2b, one observes an overall reduction in the porosity f as a function

of $\bar{\varepsilon}_e$, except in the case of the Lode angle $\theta = 60^\circ$. Furthermore, as shown in part (c), w_1 can become significantly low for all values of θ . Moreover, as shown in part (d), w_2 decreases very fast for all values of θ except for $\theta = 60^\circ$, as expected. This suggests that a void collapse mechanism (i.e., flattened cracks) is developed with increasing strain, which is also the mechanism in the context of low stress triaxiality for porous materials with isotropic matrix (see Danas and Aravas [2012]). This observation is not surprising since a BCC single crystal possesses a high number of slip systems ($K = 48$) and thus, its response is intuitively expected to be “closer” to an isotropic one.

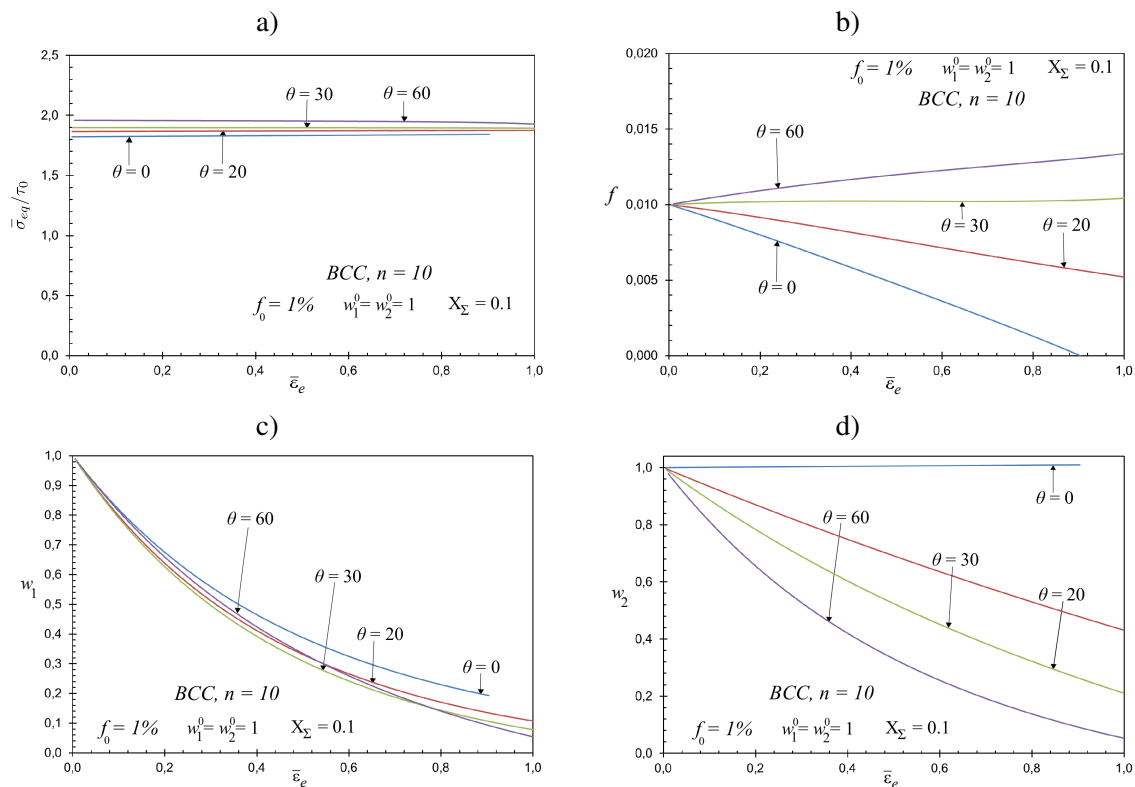


Figure 2: Plots of the MVAR estimates in the context of a porous BCC single crystal, for (a) the equivalent stress $\bar{\sigma}_e$, (b) the porosity f , and the aspect ratios (c) w_1 and (d) w_2 as a function of the equivalent strain $\bar{\varepsilon}_e$, for a low value of the stress triaxiality ($X_\Sigma = 0.1$) and four values of the Lode angle. The creep exponent is $n = 10$ and the voids are initially spherical, with a porosity $f_0 = 1\%$.

On the other hand, Fig. 3 presents MVAR plots of (a) the equivalent stress $\bar{\sigma}_e$ and (b) the porosity f as a function of the equivalent strain $\bar{\varepsilon}_e$, for a HCP single crystal with $K = 3$ and $K = 12$ slip systems, a creep exponent $n = 10$, a Lode angle $\theta = 60^\circ$ and a low value of the stress triaxiality ($X_\Sigma = 0.1$). As we can see in Fig. 3b, the porosity slightly increases for the HCP porous crystal with $K = 12$ (basal, prismatic and pyramidal Π_2) active slip systems while it doesn't evolve for the HCP crystal with $K = 3$ basal active slip systems, since such single crystal exhibits an incompressible overall response. This result is consistent with those observed in Chao et al. [2016].

4 Conclusions

A porous viscoplastic model has been developed for single crystals comprising general ellipsoidal voids at finite strains, for arbitrary orientation subjected general loading conditions. In the present framework, the microstructure evolves on average to ellipsoidal voids in time with different shape and orientation.

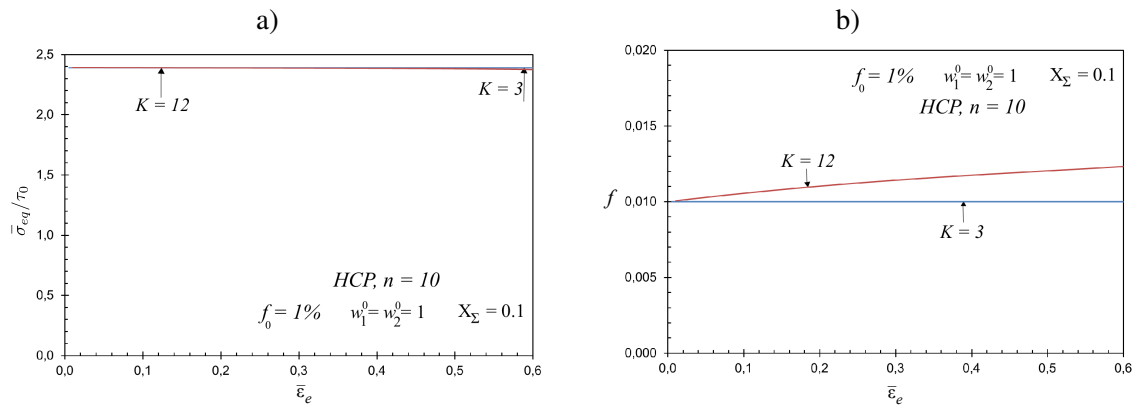


Figure 3: Plots of the MVAR estimates in the context of a porous HCP single crystal with $K = 3$ and $K = 12$ slip systems, for (a) the equivalent stress $\bar{\sigma}_e$ and (b) the porosity f as a function of the equivalent strain $\bar{\epsilon}_e$, for a low value of the stress triaxiality ($X_\Sigma = 1$) and a Lode angle $\theta = 60^\circ$. The creep exponent is $n = 10$ and the voids are initially spherical, with a porosity $f_0 = 1\%$.

In order to achieve this goal, the instantaneous effective behavior proposed in Mbiakop et al. [2015b,c] is extended with evolution laws for the internal microstructural variables used to describe the volume fraction, shape and orientation of the voids. To the best knowledge of the authors, the proposed macroscopic model is the first attempt in the literature for porous single crystals containing general ellipsoidal voids at finite strains.

Few predictions have then been provided for a large range of material parameters in the context of porous single crystals subjected to general loading conditions. More precisely, an investigation of the several microstructural mechanisms has been carried out at low triaxiality regime for several crystal structure (BCC, HCP). Then, a void collapse mechanism (i.e., flattened cracks) developed with increasing strain was found as the dominant mechanism at low stress triaxiality while it is well known that the evolution of porosity was the main softening mechanism in the high triaxiality context, leads to “high-triaxiality coalescence” of the voids.

At low stress triaxialities, the effect of the Lode angle was critical in the evolution of the porosity and the void shapes. In addition, for highly anisotropic crystals such as the three basal active slip systems in certain HCP crystal structure, the porous crystal was fully incompressible response, even if the void aspect ratios evolve. Such result is consistent with those observed in Chao et al. [2016].

Moreover, it will be useful to assess the accuracy of the MVAR predictions of the evolution of the shape and the orientation of the voids through numerical simulations. Indeed, it is well known that crystallographic aspects of plastic deformation around holes significantly affect their growth rate and in general the microstructural evolution (Srivastava and Needleman [2012]). Such validation will give us ideas in order to study coalescence of voids for arbitrary loading conditions.

As another remark, the “MVAR” model has been applied in the context of porous single crystals with viscoplastic and ideally-plastic matrix phase. Nevertheless, in real life applications, the mechanical behavior of the materials under consideration exhibits also elastic effects. Consequently, it would be of great importance to be able to incorporate elastic effects in the above described models, which would allow the study of “elasto-viscoplastic” porous single crystals.

In addition to the elasticity effects, one should also introduce the possible development of instabilities, i.e. localization to failure (see for instance Danas and Ponte Castañeda [2012]). Thus, we would be

able to treat more realistic problems such as metal ductile fracture and fatigue at the level of the grains. In the case of fatigue, a non-monotonic load is applied leading to unloading and unstable behaviors in the porous single crystal. As a first step, an investigation of the effect of cyclic loading conditions and finite deformations upon microstructure evolution and material softening/hardening using finite element (FEM) periodic unit-cell calculations has been carried out with 3D geometry at small and large number of cycles (Mbiakop et al. [2015a]). Then, as it has been the case for isotropic materials (see Danas and Aravas [2012]), the MVAR could then be implemented to standard finite element packages for solving real life applications such as rolling or extrusion of metals, ductile fracture, necking of specimens or mechanical behavior of Lotus-type metals for biological applications.

References

References

- A. Benzerga and J.B. Leblond. Ductile fracture by void growth to coalescence. *Adv. Appl. Mech.*, 44: 169–305, 2010.
- A. Benzerga, J. Besson, and A. Pineau. Anisotropic ductile fracture. part ii: Theory. *Acta Metall.*, 52:4639–4650, 2004.
- C. Chao, J. Besson, J. Forest, B. Tanguy, F. Latourte, and E. Bosso. An elastoviscoplastic model for porous single crystals at finite strains and its assessment based on unit cell simulations. *International Journal of Plasticity*, 84:58–87, 2016.
- Y.F. Dafalias. *J. App. Mech.*, 52:865–871, 1985.
- K. Danas and N. Aravas. Numerical modeling of elasto-plastic porous materials with void shape effects at finite deformations. *Composites: Part B*, 43:2544–2559, 2012.
- K. Danas and P. Ponte Castañeda. A finite-strain model for anisotropic viscoplastic porous media: I-theory. *Eur. J. Mech. A/Solids*, 28:387–401, 2009.
- K. Danas and P. Ponte Castañeda. Influence of the lode parameter and the stress triaxiality on the failure of elasto-plastic porous materials. *Int. J. Solids Struct.*, 49:1325–1342, 2012.
- J.D. Eshelby. The determination of the elastic field of an ellipsoidal inclusion and related problems. *Proc. R. Soc. Lond. A*, 241:376–396, 1957.
- Y. Gan and J. Kysar. Cylindrical void in a rigid-ideally plastic single crystal iii: hexagonal close-packed crystal. *Int. J. Plasticity*, 23:592–619, 2007.
- A.L. Gurson. Continuum theory of ductile rupture by void nucleation and growth. *J. Eng. Mater. Tech.*, 99:2–15, 1977.
- X. Han, J. Besson, S. Forest, B. Tanguy, and S. Bugat. A yield function for single crystals containing voids. *International Journal of Solids and Structures*, 50:2115–2131, 2013.
- M. Idiart and P. Ponte Castañeda. Variational linear comparison bounds for nonlinear composites with anisotropic phases. ii. crystalline materials. *Proc. R. Soc. A*, 463:925–943, 2007.

- S.M. Keralavarma, S. Hoelscher, and A.A. Benzerga. Void growth and coalescence in anisotropic plastic solids. *Int. J. Solids Struct.*, 48:1696–1710, 2011.
- B. Kondori and A.A. Benzerga. Effect of stress triaxiality on the flow and fracture of mg alloy az31. *Metallurgical and Materials Transactions A*, 45:3292–3307, 2014a.
- B. Kondori and A.A. Benzerga. Fracture strains, damage mechanisms and anisotropy in a magnesium alloy across a range of stress triaxialities. *Experimental Mechanics*, 54:493–499, 2014b.
- K. Madou and J.B. Leblond. Numerical studies of porous ductile materials containing arbitrary ellipsoidal voids - ii: Evolution of the length and orientation of the void axes. *European Journal of Mechanics A/Solids*, 42:490–507, 2013.
- A. Mbiakop, A. Constantinescu, and K. Danas. On void shape effects of periodic elasto-plastic materials subjected to cyclic loading. *European Journal of Mechanics and Solids*, 49:481–499, 2015a.
- A. Mbiakop, A. Constantinescu, and K. Danas. A model for porous single crystals with cylindrical voids of elliptical cross-section. *Int. J. Solids Struct.*, 64-65:100–119, 2015b.
- A. Mbiakop, A. Constantinescu, and K. Danas. An analytical model for porous single crystals with ellipsoidal voids. *Journal of the Mechanics and Physics of Solids*, 84:436–467, 2015c.
- F. Mc Clintock. A criterion for ductile fracture by the growth of holes. *J. App. Mech.*, 35:363–371, 1968.
- J. Paux, L. Morin, R. Brenner, and D. Kondo. An approximate yield criterion for porous single crystals. *Eur. J. Mech. A/Solids*, 51:1–10, 2015.
- P. Ponte Castañeda. Effective properties in power-law creep. *Mechanics of creep brittle materials*, 2: 218–229, 1991.
- P. Ponte Castañeda. Second-order homogenization estimates for nonlinear composites incorporating field fluctuations: I-theory. *Journal of the Mechanics and Physics of Solids*, 50:737–757, 2002.
- P. Ponte Castañeda and M. Zaidman. Constitutive models for porous materials with evolving microstructure. *J. Mech. Phys. Solids*, 42:1459–1497, 1994.
- J.R. Rice and D.M. Tracey. On the ductile enlargement of voids in triaxial stress fields. *J. Mech. Phys. Solids*, 17:201–217, 1969.
- A. Srivastava and A. Needleman. Porosity evolution in a creeping single crystal. *Model. Simul. Mater. Sci. Eng.*, 20, 2012.
- A. Srivastava, S. Gopagani, A. Needleman, V. Seetharaman, A. Staroselsky, and R. Banerjee. Effect of specimen thickness on the creep response of a ni-based single-crystal superalloy. *Acta Materialia*, 60:5697–5711, 2012.
- V. Tvergaard and A. Needleman. Analysis of the cup-cone fracture in a round tensile bar. *Acta Metall.*, 32:157–169, 1984.
- J.R. Willis. Bounds and self-consistent estimates for the overall properties of anisotropic composites. *J. Mech. Phys. Solids*, 25:185–202, 1977.